ECGS & ESC/EAEE Workshop
Earthquake and Induced Multi-Risk Early Warning and Rapid Response, 18-20 November 2015, Luxemburg

POLITECHNIKA OPOLSKA
Faculty of Civil Engineering Opole University of Technology, POLAND

INVESTIGATIONS OF THE APPLICATION OF MODERN ROTATION RATE SENSORS IN ON-LINE MONITORING OF STIFFNESS VARIATIONS OF STRUCTURES

Zbigniew ZEMBATY, Seweryn KOKOT, Piotr BOBRA, Opole University of Technology, Opole, POLAND, e-mail: z.zembaty@po.opole.pl

1. Introduction

An important area of early warning and rapid post-earthquake response is fast determination of structural damages. Traditionally it is carried out by inspections of the buildings. For some time however new methods of Structural Health Monitoring (SHM) emerged (e.g. Doebling et al. 1996), which can serve for much faster damage assessments, or even raising alarms on-line (while the structures are still shaking). Respective fast solutions of difficult inverse tasks constitute challenging problems in structural dynamics. Various interesting methods for direct seismic damage detection in buildings are under intensive investigations (see e.g. Rahmani, Todorovska, 2014).

One of key obstacles in the effective implementation of vibration based damage detection of civil infrastructure, very often built as reinforced concrete (R/C) buildings, derives from the fact of unclear damage definition of the R/C structures since they exhibit multiple cracks during various levels of vibrations (e.g. Maek, DeRoeck, 1999, Ndambi et al., 2002, Zembaty et. al 2006) and are designed to be exploited partly cracked. For these reasons special methods of their stiffness monitoring were formulated in the literature, based e.g., on fiber optics placement in the R/C beams and columns (Goldfeld, Klar, 2013).

Recently, new rotational sensors emerged in geophysics (Lee et al. 2009, Igel et al. 2012) prompting fast development of a new area of the rotational seismology. These techniques are also employed in other branches of engineering (Maydan) and angle resolutions reached level of 10^{-3} degree. Thus the new sensors can also be beneficial in the SHM of civil engineering structures (Kokot Zembaty 2009, Shreiber et al. 2009, Zembaty et al 2013).

The purpose of this paper is to report on recent research on the application of rotation rate sensors in stiffness "reconstructions" of beams, aiming at future, better monitoring of the R/C structures.

2. Problem formulation

Consider R/C structure in flexural vibrations (Fig. 1) and seismic excitations $U(t)$ (Fig. 2):

Fig. 1 Cracked reinforced-concrete beam in flexural vibrations

The stiffness of structural members and level of structural damage can be described by the intensity of cracks appearing in the beam of Fig. 1 and in the columns of the structure shown in Fig. 2. Since (due to appearance of cracks) it is difficult to directly measure strains of the R/C beam or column, by putting rotation sensor in the most bended areas of the structure one can much better follow its stiffness variations than by direct application or traditional acceleration sensors. In addition, for such structures like the ones from Fig. 2, a difficult task of monitoring

their inter-story drift during seismic excitations can directly be carried out (Schreiber et al, 2009) as the angle φ_i translates directly into the inter-story drift.

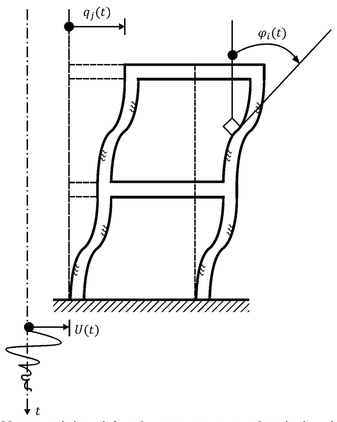

Fig. 2 Moment resisting reinforced-concrete structure under seismic excitations

Before any serious tests of the real R/C structures are carried out, the application of the rotation rate sensors in measuring the beams in bending in laboratory scale should be carried out. For these reasons experiments on plexi beams using relatively small and simple Horizon 100-100 sensors were carried out. The results are reported in chapters 4 and 6. First however basic relations between the beam axis rotation and its strains will be studied in detail.

3. Beam under flexural vibrations and the rotation of its axis

Consider equation of motion of a uniform cantilever beam ($EJ(x)=EJ=const$, $m(x)=m=const$) under kinematic excitations (Fig. 3):

$$EJ\left[\frac{\partial^4 w}{\partial x^4}+\kappa\frac{\partial^4 w}{\partial x^4}\dot{w}\right]+\mu m\dot{w}+\mu m\ddot{w}=-m\ddot{u}(t) \tag{1}$$

where 'dot' stands for differentiation with respect to time, $\ddot{u}(t)$ is the acceleration of the kinematic motion of the beam, κ, μ are constants reflecting the participation of the damping proportional to stiffness and mass respectively.

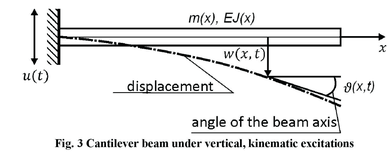

Fig. 3 Cantilever beam under vertical, kinematic excitations

Applying mode superposition method (e.g. Chopra, 2011) leads to following solution

$$w(x,t)=-\sum_{j=1}^{\infty}\wp_j\psi_j(x)\int_{-\infty}^{\infty}h_j(\tau)\ddot{u}(t-\tau)d\tau \tag{2}$$

in which

$$\wp_j=\frac{\int_0^L\psi_j(x)dx}{\int_0^L\psi_j^2(x)dx} \tag{3}$$

is the modal participation factor, $\psi_j(x)$ stands for the "j-th" mode shape, while $h_j(t)$ is the impulse response function of the "j-th" natural mode of vibration:

$$h_j(t)=\frac{1}{\omega_{jd}}\exp\left[-\xi_j\omega_j t\right]\sin\left(\omega_{jd}t\right) \tag{4}$$

where $\omega_{jd}=\sqrt{(1-\xi_j^2)}$ is the damped natural frequency and $\xi_j=\mu/(2\omega_j)+\kappa\omega_j/2$ is the modal damping ratio. Equation (2) can be used to obtain its spatial derivative i.e. the angle of the axis rotation:

$$\vartheta(x,t)=\frac{\partial w(x,t)}{\partial x}=-\sum_{j=1}^{\infty}\wp_j\psi_j'(x)\int_{-\infty}^{\infty}h_j(\tau)\ddot{u}(t-\tau)d\tau \tag{5}$$

and second derivative, which is proportional to bending moment

$$\vartheta'(x,t)=\frac{\partial^2 w(x,t)}{\partial x^2}=\frac{M}{EJ}=\frac{1}{\rho}=-\sum_{j=1}^{\infty}\wp_j\psi_j''(x)\int_{-\infty}^{\infty}h_j(\tau)\ddot{u}(t-\tau)d\tau \tag{6}$$

Using the Fourier transform one may re-write equation (2) in frequency domain as follows

$$W(x,\omega)=-\sum_{j=1}^{\infty}\wp_j\psi_j H_j(\omega)U_{accel}(\omega) \tag{7}$$

where $H_j(\omega)$ stands for frequency response function of the "j-th" mode of vibration

$$H_j(\omega)=\int_{-\infty}^{\infty}\ddot{u}(\tau)e^{-i\omega\tau}d\tau=\frac{1}{\omega_j^2-\omega^2+2i\xi_j\omega_j\omega} \tag{8}$$

in which $i=\sqrt{(-1)}$ and $U_{accel}(\omega)$ denotes Fourier transform of the excitation accelerations $\ddot{u}(t)$

$$U_{accel}(\omega)=\int_{-\infty}^{\infty}\ddot{u}(\tau)e^{-i\omega\tau}d\tau \tag{9}$$

In case of steady-state vibrations the minus signs in formulas (1, 5, 7) can be dropped. Applying the rules of time and spatial differentiation of formula (2) into its frequency domain form (7), one can obtain velocity of the angle of the beam axis $\dot{\vartheta}$ denoted in frequency domain as θ_{vel}:

$$\theta_{vel}(x,\omega)=\sum_{j=1}^{\infty}\wp_j\psi_j'(x)i\omega H_j(\omega)U_{accel}(\omega) \tag{10}$$

Assume now that the beam has a rectangular $b\times h$ cross-section. For such the Euler-Bernoulli beam the maximum strain (on the beam surface) equals

$$\varepsilon=\pm\frac{h}{2}\frac{\partial^2 w}{\partial x^2} \tag{11}$$

Thus applying eq. (5) the maximum strain can be obtained in frequency domain as follows

$$\varepsilon(x,\omega)=\pm\frac{h}{2}\sum_{j=1}^{\infty}\wp_j\psi_j''(x)H_j(\omega)U_{accel}(\omega) \tag{12}$$

Comparing equation (12) with (10) gives formula for the beam surface strain in terms of rotational velocity written in frequency domain

$$\varepsilon(x,\omega)=\theta_{vel}(x,\omega)\frac{h}{2i\omega}\frac{\sum_{j=1}^{\infty}\wp_j\psi_j''(x)H_j(\omega)}{\sum_{j=1}^{\infty}\wp_j\psi_j'(x)H_j(\omega)} \tag{13}$$

For harmonic vibrations one may substitute amplitude of rotation rate am (θ_{vel}) obtaining phase shifted maximum strain. Thus the final formula to be used in the comparisons of the amplitude of rotation rate and the amplitude of maximum strain takes form

$$am(\varepsilon)=|\varepsilon(x,\omega)|=am(\theta_{vel})\frac{h}{2}\left|\frac{1}{i\omega}\frac{\sum_{j=1}^{\infty}\wp_j\psi_j''(x)H_j(\omega)}{\sum_{j=1}^{\infty}\wp_j\psi_j'(x)H_j(\omega)}\right| \tag{14}$$

4. Experiment 1: Obtaining strain from rotational velocity of the beam axis

The small scale, laboratory models to study structural rotations should be chosen in such a way, that the resulting rotations are large enough to represent typical rotations of structures in full scale. After an analysis what was available, it was decided to perform experiments on small span, cantilever beams made of plexiglass excited by kinematic harmonic excitations. It should be noted that such small beams are much easier to excite in laboratory conditions by using kinematic excitation, than exerting the actuator motion on them. For this reason a heavy, long span, simply supported steel beam was prepared to act as a support for the analysed plexiglass beam. The steel beam was excited in vertical direction by the actuator controlled by HBM Instron system, while the analysed, plexiglass beam was clamped at the mid-span of the steel beam. This solution made it possible to excite kinematic vibrations of the plexiglass beam. To measure rotations the Systron Donner sensor HZ-100-100 ($\pm100^0$/s range) was applied. The harmonic motion of the actuator was controlled by Instron system, while data acquisition was done by multi-channel system „MCG Plus" of Hottinger. The material data of plexiglass are as follows: density $\rho = 1318.7 kg/m^3$ and Young modulus E = 4.51 GPa.

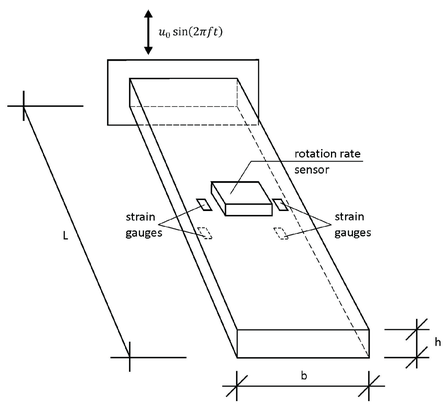

Fig. 4 Schematic view of the plexi beam under vertical, harmonic, kinematic excitations with four gauges and rotational sensor mounted in its mid span

6. Experiment 2: Reconstruction of stiffness variations of a cantilever beam

The tests were carried out using the same experimental set up as previously, but with two types of plexiglass beams: the 'intact' beam and a beam with three drops of stiffness (Fig. 7).

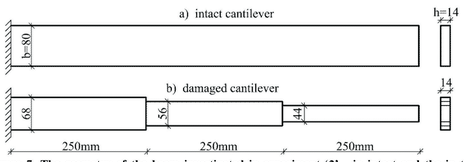

Figure 7. The geometry of the beam investigated in experiment '2' - in intact and the in the 'damaged' state defined by three stiffness reductions.

To measure translational vibrations three miniature accelerometers PCB 333B52 were installed underneath the beam. The angular motions were measured using three rotation rate sensors HZ 100-100 installed on top of the beam. All sensors were glued at points corresponding to the nodes of the finite element. The mass losses from the reductions of the beam cross-sections were compensated by gluing nuts to the beam (see Fig. 8).

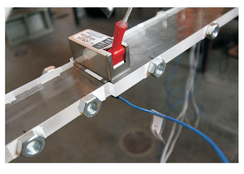

Figure 8. Detail of the beam with angular sensor HZ 100-100 installed at the beam stiffness drop and the additional, compensating masses (nuts)

The detailed scheme of the vibrating beam together with all the translational and rotational degrees of freedom is shown in Fig. 9. Two models of the 750mm long plexiglass beam were measured and analysed: the first „intact" one, with constant cross section b=80mm and h=14mm (see upper part of Fig. 7) and the second, „damaged" one, with decreased cross sections (see lower part of Fig. 5), leading to 15% drops of stiffness.

In Tab. 1 selected results of this experiment are shown.

Tab. 1 Comparison of measured and calculated amplitudes of rotation rates and strains.

frequency	amplitude of excitation accelerations	amplitude of rotation rate	amplitude of strains		
			measured	calculated (eq. 14 and column 3 as input)	calculated using FEM
[Hz]	[m/s^2]	[deg/s]			
1	2	3	4	5	6
4.50	0.5454	2.70	1.45E-05	1.37E-05	1.36E-05
5.25	0.7727	6.88	3.14E-05	3.07E-05	3.05E-05
5.70	0.9655	12.85	5.91E-05	5.36E-05	5.58E-05

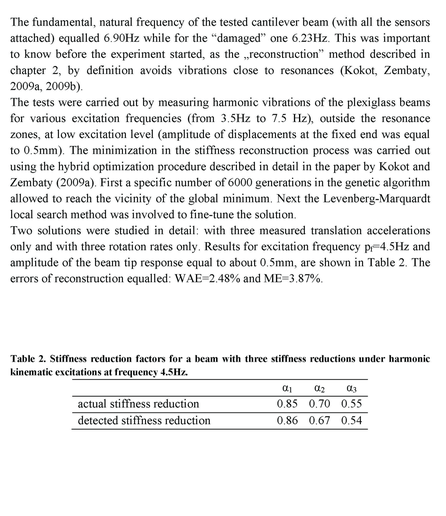

Fig. 5 Illustration of the experimental set-up to measure rotations and strains

The differences among the strains obtained from rotation rate and directly measured reached about 5-9% which can be explained by the differences between simplified, continuous dynamic model of the cantilever beam and its actual experimental realization as well as various forms of noises present in this experiment.

5. Reconstruction of flexural stiffness of a beam under harmonic vibrations from the rotations of its axis

Consider familiar equation of motion of a discrete dynamic system under harmonic excitations with frequency p [rad/s] and vector of excitation amplitudes $\mathbf{P}_0$:

$$\mathbf{M}\ddot{\mathbf{q}}+\mathbf{K}^d\mathbf{q}=\mathbf{P}_0e^{ipt} \tag{15}$$

where superscript 'd' indicates that the structure vibrates in a 'damaged' state with its original, stiffness matrix $\mathbf{K}$ reduced to $\mathbf{K}^d$ due to the accumulated damages, while the matrix of inertia $\mathbf{M}$ stays unchanged. It is also assumed that structural response is small and out of the resonance frequencies zones, so that damping effects may be neglected. Such situation occurs for example for the cracked reinforced concrete structures (e.g. Zembaty et al., 2006). In Fig. 6, a fragment of a beam structure under harmonic excitations is presented. The structure is divided into finite elements k-1, k, k+1 etc. The generalized coordinates q_i, q_{i+1}, q_{i+2}, are assumed along the measurement directions and include also rotational degrees of freedom.

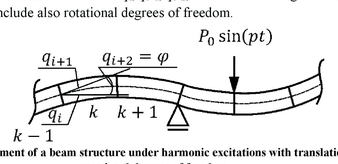

Figure 6. Fragment of a beam structure under harmonic excitations with translational and rotational degrees of freedom

Eq. (15) can be solved using familiar algebraic matrix equation with respect to the unknown response amplitude vector u:

$$\left(\mathbf{K}^d-p^2\mathbf{M}\right)\mathbf{u}=\mathbf{P}_0 \tag{16}$$

The global stiffness matrix can calculated using the Finite Element Method (FEM) with contributions from all respective finite elements:

$$\mathbf{K}^d=\sum_{i=1}^{n}\mathbf{K}_i^{de}=\sum_{i=1}^{n}\alpha_i\mathbf{K}_i^{ue} \tag{17}$$

where n is the number of all discretized elements. At this stage one can introduce the key parameters of this analysis which are non-dimensional stiffness reduction factors α_i which describe relative stiffness loss due to accumulated damages ($0\le\alpha_i\le1$). Substituting eq.17 into eq. 16 one obtains:

$$\left(\sum_i^n\alpha_i\mathbf{K}_i^{ue}-p^2\mathbf{M}\right)\mathbf{u}=\mathbf{P}_0 \tag{18}$$

Eq. 18 can be applied to find the vector of the amplitudes of displacements **u** in terms of the vector of driving force amplitudes $\mathbf{P}_0$, when the FEM model of the structure is prepared.

Consider now the norm J measuring difference between vectors of the amplitudes $\mathbf{u}^c$ calculated using Finite Element Method and the vector of amplitudes $\mathbf{u}^m$ measured in the actual structure:

$$J(\boldsymbol{\alpha})=\sum_{j=1}^{n_d}\left(\frac{u_j^c(\boldsymbol{\alpha})-u_j^m}{u_j^m}\right)^2 \tag{19a}$$

where n_d is the number of measured displacement amplitudes. Finding minimum of eq. 19a the vector of stiffness reduction factors $\boldsymbol{\alpha}$ describing the actual state of damage can be obtained. This reconstruction procedure requires the structure to be excited and to acquire all the amplitudes along dynamic degrees of freedom of the structure. Classic FEM analysis of beams and frames defines structural response usually only in terms of translational coordinates, while the rotational degrees of freedom are removed from the global stiffness matrix by static condensation. Thus one can easily include rotational coordinates in the analyses by keeping selected, required rotational degrees of freedom (not condensing them out). In this case instead of equation (19a) we will have

$$J_{dr}(\boldsymbol{\alpha})=\sum_{j=1}^{n_{dr}}\left(\frac{u_j^c(\boldsymbol{\alpha})-u_j^m}{u_j^m}\right)^2 \tag{19b}$$

where n_{dr} denotes the number of translational and additional, rotational degrees of freedom. A comparison of the effectiveness of minimization of functionals given by Eq. (19a) or (19b) using Genetic Algorithms and Levenberg-Margquardt local search (GA L-M) was subject of a detailed numerical analysis in the paper by Kokot and Zembaty (2009b). When analyzing reconstructions of multiple stiffness two measures of its effectiveness can be defined:

- Weighted Average Error (WAE):.

$$\mathrm{WAE}=\sqrt{\sum_{i=1}^{n_c}\left(\frac{\alpha_i^a-\alpha_i^d}{\alpha_i^d}\right)^2} \tag{20}$$

measuring averaged difference between computed and assumed vectors of stiffness reduction factors (the averaging summation takes place over all the discretized elements n_c.

- Maximum Error (ME) between actual and measured stiffness distribution:

$$\mathrm{ME}=\max_i\left|\alpha_i^a-\alpha_i^d\right| \tag{21}$$

The above symbols α_i with superscripts a and d denote respectively the 'assumed' and 'detected' stiffness losses.

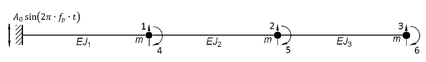

Figure 9. Dynamic model of the cantilever beam vibrating under vertical, kinematic, harmonic excitations

The fundamental, natural frequency of the tested cantilever beam (with all the sensors attached) equalled 6.90Hz while for the "damaged" one 6.23Hz. This was important to know before the experiment started, as the „reconstruction" method described in chapter 2, by definition avoids vibrations close to resonances (Kokot, Zembaty, 2009a, 2009b).

The tests were carried out by measuring harmonic vibrations of the plexiglass beams for various excitation frequencies (from 3.5Hz to 7.5 Hz), outside the resonance zones, at low excitation level (amplitude of displacements at the fixed end was equal to 0.5mm). The minimization in the stiffness reconstruction process was carried out using the hybrid optimization procedure described in detail in the paper by Kokot and Zembaty (2009a). First a specific number of 6000 generations in the genetic algorithm allowed to reach the vicinity of the global minimum. Next the Levenberg-Marquardt local search method was involved to fine-tune the solution.

Two solutions were studied in detail: with three measured translation accelerations only and with three rotation rates only. Results for excitation frequency p_f=4.5Hz and amplitude of the beam tip response equal to about 0.5mm, are shown in Table 2. The errors of reconstruction equalled: WAE=2.48% and ME=3.87%.

Table 2. Stiffness reduction factors for a beam with three stiffness reductions under harmonic kinematic excitations at frequency 4.5Hz.

	α_1	α_2	α_3
actual stiffness reduction	0.85	0.70	0.55
detected stiffness reduction	0.86	0.67	0.54

7. Conclusions

This paper reports the results of early stage, laboratory experiments of the application of modern rotation rate sensors to measure and monitor of structural vibrations in civil and seismic engineering. Following positive recommendations from numerical simulations (Abdo, Hori, 2002, Kokot, Zembaty, 2009b), both experiments demonstrated the ability of modern rotation rate sensors to be effectively applied in measuring structural vibrations and in difficult, stiffness "reconstructions" of practical structural health monitoring.

This is a good prognostic for future application of rotation rate sensors not only to directly measure rotations of key structural elements, but also to follow strains and monitor distributed damages of some civil engineering structures, particularly the difficult to monitor, moment resisting reinforced concrete frames and multi-story buildings requiring inter-story drift to measure.

More details about the reported experiments can be found in the recent paper by Zembaty et al. (2013).

Acknowledgments This research was supported in part by the Polish NSF Grant N506 289037 „Simulation and experimental investigations of rotation measurements in dynamic identification of bar structures" and statutory fund of Polish Ministry of Science and Higher Education (NBS 15/14). The Authors wish to thank dr Bronisław Jędraszak (Opole University of Technology) and Dariusz Knapek (EC Test Systems, Cracow) for their assistance in carrying out the experiments.

References

Chopra AK (2011) *Dynamics of Structures*, Theory and Application to Earthquake Engineering. Prentice Hall, New Jersey

Doebling SW, Farrar CR, Prime MB, Shevitz DW. (1996). Damage identification and health monitoring of structural and mechanical systems from changes in their vibration characteristics: a literature review, Report LA-13070-MS, Los Alamos

Goldfeld, Y., Klar A. (2013) Damage identification in reinforced concreto beams using spatially distributed strain measurements, *Journal of Structural Engineering* ASCE, vol.139, no. 1

Igel H., Brokesova J., Evans J. and Zembaty Z. (2012), Preface to special issue on "Advances in rotational seismology: instrumentation, theory, observations and engineering", *Journal of Seismology*, vol.16, 571-72

Kokot S, Zembaty Z., (2009a), Damage reconstruction of 3d frames using genetic algorithms with Levenberg-Marquardt local search. *Soil Dynamics and Earthquake Engineering*, vol.29, pp.311-323

Kokot S. and Zembaty Z., (2009b), Vibration based stiffness reconstruction of beams and frames by observing their rotations under harmonic excitations - a numerical analysis, *Engineering Structures*, vol.31, pp.1581-1588

Lee W.H.K., Celebi M., Igel H., Todorovska M. (2009), Introduction to the Special Issue on Rotational Seismology and Engineering Applications, *BSSA*, vol. 99(2B)

Maeck J., De Roeck G., (1999) Dynamic bending and torsional stiffness derivation from modal curvatures and torsion rates, *Journal of Sound and Vibration*, vol. 225, 1999, pp.153–170

Meydan T, (1997) Recent trends in linear and angular accelerometers. *Sensors and Actuators A Physical*, vol. 59, pp. 43-50

Ndambi, J.-M., Vantomme, J., Harri, K., Damage assessment in reinforced concrete beams using eigenfrequencies and mode shape derivatives, *Engineering Structures*, vol. 24, 2002, pp. 501-515.

Schreiber K. U., Velikoseltsev A., Carr A.J. and Franco-Anaya R. (2009), The Application of Fiber Optic Gyroscopes for the Measurement of Rotations in Structural Engineering, *BSSA*, vol.99, pp.1207-1214,

Rahmani M., Todorovska MI (2014). Structural Health Monitoring of a 54-story Steel Frame Building-Wave and Vibrational Characteristics during Five Earthquakes, *Earthquake Spectra*, vol. 31, No. 1, pp. 501-525.

Zembaty Z., Kowalski M., Pospisil S., Dynamic identification of a reinforced concrete frame in progressive states of damage, *Engineering Structures*, vol.28, 2006, pp. 668-681.

Zembaty Z., Kokot S. and Bobra P. (2013), Application of rotation rate sensors in an experiment of stiffness 'reconstruction', *Smart Materials & Structures*, vol. 22, open access link: http://iopscience.iop.org/0964-1726/22/7/07700